Molecular Organization of an Amphiphilic Styryl Pyridinium Dye in Monolayers at the Air/Water Interface in the Presence of Various Anions

Andrey A. Turshatov,*,† Dietmar Möbius,† Mariano L. Bossi,*,† Stefan W. Hell,† Artem I. Vedernikov,‡ Natal'ya A. Lobova,‡ Sergey P. Gromov,‡ Michael V. Alfimov,‡ and Sergey Yu. Zaitsev§

Department of NanoBiophotonics, Max-Planck-Institute for Biophysical Chemistry, 37070 Göttingen, Germany, Photochemistry Center, Russian Academy of Sciences, Novatorov Str. 7a, Moscow 119421, Russia, and Moscow State Academy of Veterinary Medicine and Biotechnology, Acad. Skryabina Str. 23, Moscow 109472, Russia

Received July 19, 2005. In Final Form: November 12, 2005

Amphiphilic 4-(3′,4′-dimethoxystyryl)-*N*-octadecylpyridinium perchlorate and bromide form stable monolayers at the air/water interface. Small differences in the surface pressure−area and surface potential−area isotherms depending on the anion indicate interactions between the chromophore and the anions on the pure water subphase. The monolayer behavior is considerably modified on 10 mM aqueous solutions of KI, $KClO_4$, KCl, and KF as revealed by isotherm measurements, reflection spectroscopy, and Brewster angle microscopy. The phase transition observed in the isotherms is shifted to higher surface pressure because of variation of the salt according to the Hofmeister series. Upon monolayer compression, the chromophores are increasingly tilted, and a shift of the band to longer wavelengths is attributed to the environment becoming less polar. However, in the case of KCl at small areas per molecule, relaxation is observed at constant area with the appearance of a new band shifted to shorter wavelengths. This band is assigned to small associates of about four chromophores (H aggregates). In the case of KI, a new band shifted to longer wavelengths is found. Theoretical calculations did not yield a transition in the observed range, even for large aggregates (J aggregates). Therefore, other interactions may be responsible for the appearance of this band.

Introduction

A class of styryl pyridinium dyes has the following particularly interesting photophysical property: a high molecular hyperpolarizability[1] that plays a key role in second-harmonic generation[2−6] as well as in the sensitivity to the environment, detectable as a solvatochromic effect[7] or as the dependence of the electrical membrane potential.[8] Furthermore, the generation of photocurrents using this type of dye has been studied in detail.[5,9]

In a large portion of the work published in these fields, amphiphilic dyes with long aliphatic chains and the Langmuir−Blodgett (LB) technique have been used to prepare nanoscale devices with external control of their properties. The substituent in the para position of the styryl fragment strongly influences the photophysical and photochemical properties of the dyes. For example, the strongly electron-donating group in aminostyryl pyridinium dyes gives rise to locally excited (fluorescent) and twisted intramolecular charge-transfer (nonfluorescent) states, whereas cis/trans isomerization is unlikely to occur in the exited state.[10] In contrast, in the absence of substituents in the styryl part, the dye shows reversible photoisomerization that has been studied in solution, crystals, micelles, and LB assemblies.[11] We have synthesized the amphiphilic dyes with two methoxy groups in the para and meta positions of the styryl part and an octadecyl substituent at the pyridinium nitrogen.

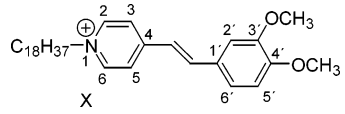

X = ClO_4^- (**dye 1**); Br^- (**dye 2**)

This dye shows reversible photoisomerization between the strongly fluorescent E isomer and the nonfluorescent Z isomer. This behavior is highly interesting with respect to new concepts of optical imaging and writing with resolution beyond the diffraction limit[12] and is the basis for the design of devices for optical information storage by switching between emitting and nonemitting states.[13,14]

The synthesized compounds also have the potential for further chemical modification by attaching an ionophore crown ether ring to the styryl part of the molecule. The synthesis and properties of such complex photochromic systems have recently been

* To whom correspondence should be addressed. E-mail: atursha@gwdg.de; mbossi@gwdg.de.
† Max-Planck-Institute for Biophysical Chemistry.
‡ Russian Academy of Sciences.
§ Moscow State Academy of Veterinary Medicine and Biotechnology.

(1) Duan, X.; Konami, H.; Okada, S.; Oikawa, H.; Matsuda, H.; Nakanishi, H. *J. Phys. Chem.* **1996**, *100*, 17780.
(2) Steinhoff, R.; Chi, L. F.; Marowsky, G.; Möbius, D. *J. Opt. Soc. Am. B* **1989**, *6*, 843.
(3) Sharath Chandra, M.; Ogata, Y.; Kawamata, J.; Radhakrishnan, T. P. *Langmuir* **2003**, *19*, 10124.
(4) Liu, X.; Liu, L.; Chen, Z.; Lu, X.; Zheng, J.; Wang, W. *Thin Solid Films* **1992**, *219*, 221.
(5) Li, F.-Y.; Jin, L.-P.; Huang, C.-H.; Zheng, J.; Guo, J.-Q.; Zhao, X.-S.; Liu, T.-T. *Chem. Mater.* **2001**, *13*, 192.
(6) Niidome, Y.; Ayukawa, H.; Yamada, S. *J. Photochem. Photobiol., A* **2000**, *132*, 75.
(7) Huang, Y.; Cheng, T.; Li, F.; Luo, C.; Huang, C. H.; Cai, Z.; Zeng, X.; Zhon, J. *J. Phys. Chem. B* **2002**, *106*, 10031.
(8) Clarke, R. J.; Lüpfert, C. *Biophys. J.* **1999**, *76*, 2614.
(9) Lang, A.-D.; Zhai, J.; Huang, C.-H.; Gan, L.-B.; Zhao, Y.-L.; Zhou, D.-J.; Chen, Z.-D. *J. Phys. Chem. B* **1998**, *102*, 1424.
(10) Kim, J.; Lee, M. *J. Phys. Chem. A* **1999**, *93*, 3378.
(11) Quina, F. H.; Whitten, D. G. *J. Am. Chem. Soc.* **1977**, *99*, 877.
(12) Hell, S. W.; Jakobs, S.; Kastrup, L. *Appl. Phys. A* **2003**, *77*, 859.
(13) Dvornikov, A. S.; Liang, Y.; Cruse, C. S.; Rentzepis, P. M. *J. Phys. Chem. B* **2004**, *108*, 8652.
(14) Irie, M. *Chem. Rev.* **2000**, *100*, 1685.

10.1021/la051942q CCC: $33.50
Published on Web 01/14/2006

published.[15] From this point of view, the styryl dyes presented here may be considered to be model compounds for the study of the organization in monolayers and of the photochemical behavior of dyes containing the additional ionophore group.

In this article, we discuss stability and association phenomena of the dyes in monolayers at the air−water interface in the presence of various anions. We investigated the effect of different anions by measuring surface pressure−area and surface potential−area isotherms as well as using reflection spectroscopy and Brewster angle microscopy (BAM). These methods, in particular, reflection spectroscopy, provide information on chromophore orientation and association in monolayers. The unattended, very strong influence of the chemical nature of anions on molecular organization and spectroscopic properties of cationic amphiphiles has caught our attention because we expect similar effects on monolayers of other cationic dyes. However, this fact is poorly discussed in the literature.

The specific influence of anions on the properties of the surface of salt solutions in the absence of an insoluble lipid monolayer is well known and is classified according to the Hofmeister series of anions. This series of anions was established in the 19th century on the basis of studies of the solubility of proteins in electrolyte solutions.[16] The translation to English of two original articles from a series of Hofmeister's works is available.[17] The following investigations showed that the Hofmeister series is applicable not only to biological phenomena but also to a wide range of interfacial phenomena including the surface properties of salt solutions,[18−20] the colloid stability of latex,[21,22] the adsorption of ionic surfactants at the air/water interface,[23−27] and the organization of octadecylamine[28] and dimethyl-dioctadecylammonium salts,[29] calixarenes,[30] and 1,2-dipalmitoyl-phosphatidylcholine in Langmuir monolayers.[31] The Hofmeister series of anions may be slightly different, depending on the studied phenomenon. In any case, one end of the sequence includes large, highly polarizable anions such as I^-, ClO_4^-, and CNS^-. The influence of these anions may be quite specific in some cases. The other end of the sequence includes ions F^-, OH^-, SO_4^{2-}, and HPO_4^{2-}. According to Ninham and Boström, the differences are related to the strength of dispersion interactions and the ion solvation energy.[32,33] The role of dehydration near the interface was also emphasized by other authors.[34−36] In addition, Monte Carlo simulations have shown that ions may cause a breakdown of the hydrogen-bond network in the vicinity of the ions,[37] but later experimental results[38,39] have shown that this effect is not very strong.

Materials and Methods

The synthesis of the dyes has been previously described.[40] After minor alterations in the precipitation procedure, we obtained the dye with two different anions: ClO_4^- (dye 1) and Br^- (dye 2). Chloroform (Baker, 99.8% purity) was used as the solvent for preparing monolayers of the dyes. All other solvents were purchased from Merck with a purity of 99.5% and were used without additional purification. All salts were purchased from Merck with a purity of 99.5% with the exception of potassium perchlorate (99+% purity), which was purchased from Sigma-Aldrich.

The surface pressure (π)−area (A) and surface potential (ΔV)−area (A) isotherms of dye monolayers were recorded on a rectangular trough made of poly(tetrafluoroethylene) with dimensions of 11 cm × 38 cm × 0.8 cm provided with a 2-cm-wide filter paper Wilhelmy balance and a vibrating plate condenser.[41] Monolayers were formed by spreading 50 μL of 1 mM chloroform solutions of dyes 1 and 2 onto water or 1 and 10 mM aqueous solutions of different salts at 20 °C. After ca. 10 min of relaxation to allow solvent evaporation, the monolayers were compressed by moving the barrier at a constant speed of about 10 cm^2/min. Reflection spectra of the monolayers at constant area were measured under the normal incidence of light with a modified spectrometer of the type described earlier[42,43] and recorded as the difference ΔR of the reflectivities on the monolayer-covered surface and the clean water surface. The trough is of the same type as that used for isotherm measurements; however, the starting surface area is smaller (289 instead of 365 cm^2) because of the separation of a reference section. The monolayers were compressed at a speed of 10 cm^2/min to the desired area per molecule, and the measurement was started without additional delay. The time required to measure a spectrum was ca. 50 s. The reflection normalized with respect to the surface density of the dye is obtained according to $\Delta R_{norm} = \Delta R \cdot A$, where A is the area per molecule. Absorption and fluorescence spectra of dyes 1 and 2 in a 10^{-5} M solution using different organic solvents were measured in a Varian Cary 4000 UV−vis spectrophotometer and a Varian Cary Eclipse fluorescence spectrophotometer.

Results

Surface Pressure−Area and Surface Potential−Area Isotherms. The π−A (solid lines) and ΔV−A (dashed lines) isotherms of dye 1 with ClO_4^- (curves 1, 1a, 3, and 3a) and dye 2 with Br^- (curves 2 and 4), respectively, on water are presented in Figure 1. When spreading a solution volume of 50 μL as usual, the area per dye before starting the compression is A = 1.17 nm^2. As can be seen, a surface pressure of about 2 mN/m and a surface potential of about 0.47 V are measured for this area for ClO_4^- as the anion. For the material with this anion, a much smaller amount has been spread such that $\pi \approx 1$ mN/m and ΔV = 0.26 V before compression, corresponding to A = 10 nm^2. (In

(15) Gromov, S. P.; Ushakov, E. N.; Fedorova, O. A.; Baskin, I. I.; Buevich, A. V.; Andryukhina, E. N.; Alfimov, M. V.; Johnels, D.; Edlund, U. G.; Whitesell, J. K.; Fox, M. A. *J. Org. Chem.* **2003**, *68*, 6115.
(16) Hofmeister, F. *Arch. Exp. Pathol. Pharmakol.* **1888**, *24*, 247.
(17) Kunz, W.; Henle, J.; Ninham, B. W. *Curr. Opin. Colloid Interface Sci.* **2004**, *9*, 19.
(18) Weissenborn, P. K.; Pugh, R. J. *J. Colloid Interface Sci.* **1996**, *184*, 550.
(19) Boström, M.; Kunz, W.; Ninham, B. W. *Langmuir* **2005**, *21*, 2619.
(20) Mucha, M.; Frigato, T.; Levering, L. M.; Allen, H. C.; Tobias, D. J. *J. Phys. Chem. B* **2005**, *109*, 7617.
(21) López-León, T.; Jódar-Reyes, A. B.; Ortega-Vinuesa, J. L.; Bastos-González, D. *J. Colloid Interface Sci.* **2005**, *284*, 139.
(22) López-León, T.; Gea-Jódar, P. M.; Bastos-González, D.; Ortega-Vinuesa, J. L. *Langmuir* **2005**, *21*, 87.
(23) Knock, M. M.; Bain, C. D. *Langmuir* **2000**, *16*, 2857.
(24) Teppner, R.; Haage, K.; Wantke, D.; Motschmann, H. *J. Phys. Chem. B* **2000**, *104*, 11489.
(25) Koelsch, P.; Motschmann, H. *Langmuir* **2005**, *21*, 3436.
(26) Warszynski, P.; Lunkenheimer, G.; Czichocki, G. *Langmuir* **2002**, *18*, 2506.
(27) Para, G.; Warszynski, P.; Jarek, E. *Colloids Surf., A* **2005**, *261*, 65.
(28) Gurau, M. C.; Lim, S.-M.; Castellana, E. T.; Albertorio, F.; Kataoka, S.; Cremer, P. S. *J. Am. Chem. Soc.* **2004**, *126*, 10522.
(29) Ahuja, R. C.; Caruso, P.-L.; Möbius, D. *Thin Solid Films* **1994**, *242*, 195.
(30) Lonetti, B.; Lo Nostro, P.; Ninham, B. W.; Baglioni, P. *Langmuir* **2005**, *21*, 2242.
(31) Aroti, A.; Leontidis, E.; Maltseva, E.; Brezesinski, G. *J. Phys. Chem. B* **2004**, *108*, 15238.
(32) Boström, M.; Ninham, B. W. *Langmuir* **2004**, *20*, 7569.
(33) Boström, M.; Ninham, B. W. *Biophys. Chem.* **2005**, *114*, 95.
(34) Jungwirth, P.; Tobias, D. J. *J. Phys. Chem. B* **2002**, *106*, 6361.
(35) Dang, L. X.; Chang, T.-M. *J. Phys. Chem. B* **2002**, *106*, 235.
(36) Karlström, G.; Hagberg, D. *J. Phys. Chem. B* **2002**, *106*, 11585.
(37) Hribar, B.; Southall, N. T.; Vlachy, V.; Dill, K. A. *J. Am. Chem. Soc.* **2002**, *124*, 12302.
(38) Batchelor, J. D.; Olteanu, A.; Tripathy, A.; Pielak, G. J. *J. Am. Chem. Soc.* **2004**, *126*, 1958.
(39) Omta, A. W.; Kropman, M. F.; Woutersen, S.; Bakker, H. J. *Science* **2003**, *301*, 347.
(40) Turshatov, A. A.; Bossi, M. L.; Möbius, D.; Hell, S. W.; Vedernikov, A. I.; Gromov, S. P.; Lobova, N. A.; Alfimov, M. V.; Zaitsev, S. Y. *Thin Solid Films* **2005**, *476*, 336.
(41) Kuhn, H.; Möbius, D.; Bücher, H. Spectroscopy of Monolayer Assemblies. In *Physical Methods of Chemistry*; Weissberger, A., Rossiter, B., Eds.; John Wiley & Sons: New York, 1972; Vol. 1, Part 3B, pp 577−702.
(42) Grüniger, H.; Möbius, D.; Meyer, H. *J. Chem. Phys.* **1983**, *79*, 3701.
(43) Orrit, M.; Möbius, D.; Lehmann, U.; Meyer, H. *J. Chem. Phys.* **1986**, *85*, 4966.

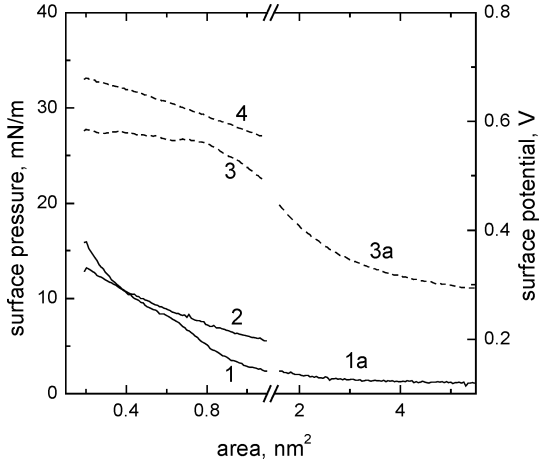

Figure 1. Surface pressure−area (1, 1a, and 2) and surface potential−area isotherms (3, 3a, and 4) on pure water: dye 1 (1, 1a, 3, and 3a) and dye 2 (2 and 4).

Figure 1, the isotherms are shown for $A < 5.5$ nm^2.) The monolayer of dye 1 on pure water shows a gradual increase in surface pressure upon compression starting at $A = 10$ nm^2 and a hardly detectable phase transition at surface pressures of about 8.3−9.0 mN/m and areas of 0.67−0.60 nm^2. The monolayer is quite stable at an area corresponding to the cross section of the molecule oriented normal to the surface (0.33 nm^2); however, upon further compression, it undergoes fast relaxation when the barrier is stopped, as indicated by a decrease in surface pressure. For dye 2 (with Br^-), the surface pressure is larger for areas $A > 0.4$ nm^2, and the transition to a liquid-condensed state is absent. This different behavior due to different counterions may be taken as evidence that the counterion is at least partially retained or trapped by the cationic amphiphile in monolayers on pure water.

The surface potential of monolayers on water of dye 1 (Figure 1, curves 3 and 3a) increases gradually from about 0.26 V at 10 nm^2 to about 0.57 V at an area of 0.4 nm^2. The replacement of ClO_4^- anions in the preparation by Br^- (dye 2) (Figure 1, curve 4) leads to an increase in the surface potential by about 50 to 100 mV in the area range presented in Figure 1.

The behavior of dye 1 is considerably modified in the presence of various salts in the aqueous subphase. The $\pi-A$ and $\Delta V-A$ isotherms of dye 1 on 10 mM solutions of KF (curves 1), KCl (curves 2), KI (curves 3), and $KClO_4$ (curves 4) are shown in Figure 2a and b, respectively. A reduction in the salt concentration to 1 mM did not markedly change the isotherms. In all cases, the $\pi-A$ isotherms indicate a more or less pronounced transition between liquid-expanded and liquid-condensed states of the monolayers. In the presence of $KClO_4$ (Figure 2a, curve 4), this transition is the most pronounced and is observed at a surface pressure of $\pi = 4$ mN/m in the area range of $0.80 \geq A \geq 0.38$ nm^2. It is remarkable that in the presence of 10 mM $KClO_4$ the surface pressure increases upon compression from almost 0 at $A = 1.17$ nm^2, whereas on water a surface pressure of 2 mN/m is observed for dye 1. Moreover, in the presence of $KClO_4$, the monolayer in the liquid-condensed state is very stable during compression from $A = 0.38$ nm^2 to collapse at $A_c = 0.24$ nm^2, resulting in a surface pressure increase to $\pi_c = 62.0$ mN/m. The replacement of $KClO_4$ into the subphase by salts in the series KI, KCl, KF leads to an increase in the surface pressure of the phase transition, which becomes less and less pronounced in this series (Figure 2a, curves 3, 2, and 1, respectively). The surface pressure of the phase transition increases from 4 mN/m ($KClO_4$) to 7, 19, and 28 mN/m at $A = 0.50$ nm^2 in the presence of KI, KCl, and KF, respectively (10 mM solutions). This sequence follows the Hofmeister series of anions. Upon further compression, the liquid-condensed phase of the dye 1 monolayers ending with collapse is clearly observed on aqueous solutions of KI ($A_c = 0.28$ nm^2, $\pi_c = 45$ mN/m) and KCl ($A_c = 0.21$ nm^2, $\pi_c = 41$ mN/m) but not in the case of KF. Monolayer stability depends on the salt. In the presence of KI and KF, the monolayers are stable and show very little surface pressure decrease with time at constant area (only a few mN/m even at high compression). In contrast, the surface pressure decreases quickly to an equilibrium surface pressure of about 15 mN/m in the presence of KCl after compression to $A = 0.24$ nm^2. For larger areas, the relaxation of the surface pressure is very similar to that observed in the presence of the other ions.

The surface potential−area isotherms shown in Figure 2b provide additional evidence for the influence of the different anions in the aqueous subphase on the behavior of the dye 1 monolayers. On 10 mM $KClO_4$, a sharp increase in the surface potential ΔV from 0 to about 250−300 mV upon compression is observed at $A = 1.0$ nm^2, and ΔV is almost constant during further compression (Figure 2b, curve 4). Quite similar behavior, but a less abrupt increase in the surface potential in the area range from 1.2 to 1.0 nm^2 upon compression, is observed for monolayers of dye 1 in the presence of 10 mM KI. Such a more or less abrupt increase in the surface potential upon compression is not observed in the case of KCl and KF (Figure 2b, curves 2 and 1, respectively), even for much larger areas (not shown here). As a result, these anions cause an overall increase in the surface potential. In addition, the surface potential increases strongly with compression in the presence of KCl for $A < 0.5$ nm^2.

Besides the characterization of monolayers by surface pressure−area and surface potential−area isotherms, spectroscopic measurements are indispensable to the understanding of the molecular organization of dye 1 in monolayers under different surface pressures in the absence and presence of various salts interacting with the chromophore.

Spectroscopic Properties of Bulk Solutions. To clarify the effects of the polarity and polarizability of the environment on the behavior of the dyes, we investigated the influence of a series of solvents on the absorption and emission spectra of dye 1 and in some cases of dye 2. The wavelengths of the absorbance and fluorescence maxima (i.e., λ_{max}(abs) and λ_{max}(em)) are listed in Table 1. In addition, the refractive index n and the dielectric permeability ϵ that are relevant to the interpretation of solvent effects are listed in this Table.

Reflection Spectroscopy. The normalized reflection spectra of monolayers of dye 1 on water for different areas A are shown in Figure 3a. At $A = 0.95$ nm^2 (curve 1), the spectrum with a maximum at $\lambda_{max} = 395$ nm and a bandwidth (fwhm) of 77 nm closely resembles the absorption spectrum in acetonitrile solution (not shown). Upon compression (i.e., with decreasing area A), the intensity ΔR_{norm} of the reflection normalized with respect to surface density decreases considerably. Furthermore, a red shift and a broadening of the band are observed with $\lambda_{max} = 410$ nm and fwhm = 101 nm at $A = 0.26$ nm^2 (curve 4). The reflection spectra of dye 1 on 10 mM aqueous $KClO_4$ solution are quite similar to those on water; see Figure 3b. Again, the intensity ΔR_{norm} decreases with decreasing area, and a shift as well as a broadening of the band is observed for areas $A \leq 0.5$ nm^2. On 10 mM aqueous KF solution, similar behavior is observed, at least for large areas A; see Figure 3c. The normalized reflection ΔR_{norm} decreases upon reduction of area A, although not to the same extent as on water and 10 mM $KClO_4$. Furthermore, there is practically no red shift and rather little broadening of the band

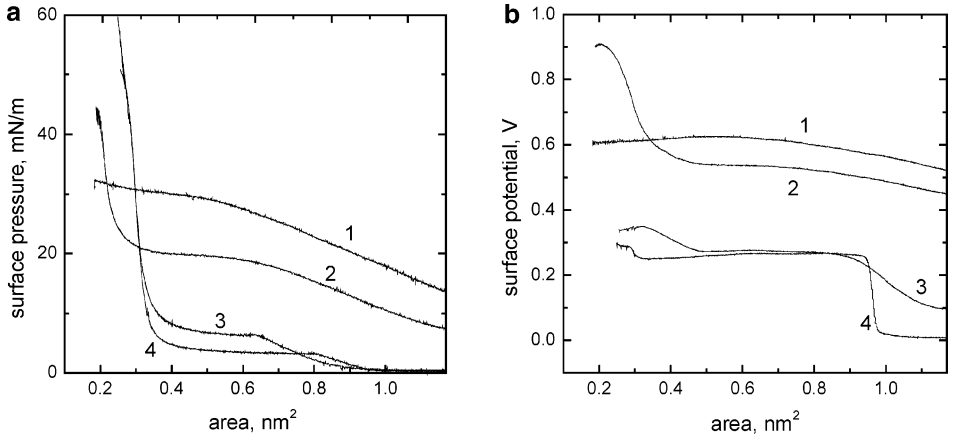

Figure 2. (a) Surface pressure−area isotherms of dye 1 on aqueous 10 mM salt subphases: KF (1), KCl (2), KJ (3), and $KClO_4$ (4). (b) Surface potential−area isotherms of dye 1 on aqueous 10 mM salt subphases: KF (1), KCl (2), KJ (3), and $KClO_4$ (4).

Table 1

solvent	n^a	ϵ^a	$\lambda(\text{abs})_{max}$	$\lambda(\text{em})_{max}$
acetonitrile	1.3416	37.5	398 (398[b])	545
ethanol	1.359	24.6	406 (406[b])	537
2-propanol	1.375	19.9	406	532
2-butanol	1.297	15.8	413	532
pyridine	1.507	12.4	415	543
chloroform	1.443	4.8	420 (414[b])	532
dichloromethane	1.421	8.9	429 (422[b])	537
tetrahydrofuran	1.405	7.6	405 (398[b])	539
ethyl acetate	1.370	6.0	399	532

[a] CRC Handbook of Chemistry and Physics, 80th ed.; Lide, D. R., Ed.; CRC Press: Boca Raton, FL, 1999. [b] Absorption maximum for dye 2 under the same conditions.The oscillator strength *f* and transition dipole moment *M* were calculated to be 0.670 and 8.744 D for acetonitrile solutions of dye 1 and 0.782 and 10.010 D, for chloroform solution, respectively.

observed from fwhm = 72 nm at $A = 0.96$ nm^2 to 85 nm at $A = 0.28$ nm^2.

More pronounced differences in this behavior are found in the presence of 10 mM KCl (Figure 4a) and KI (Figure 4b). On the KCl solution, the normalized reflection ΔR_{norm} decreases initially when decreasing the area from $A = 0.96$ nm^2 (curve 1) to 0.40 nm^2 (curve 3). However, the intensity ΔR_{norm} increases again for $A = 0.35$ nm^2 (curve 4) and 0.24 nm^2 (curve 5). Furthermore, the fwhm increases with decreasing area from 77 nm (at 0.96 nm^2) to 118 nm (at 0.24 nm^2). This broadening is much more pronounced than that observed on water and $KClO_4$. On 10 mM aqueous KI, the reflection spectra of dye 1 show the appearance of a new band with a maximum at 500 nm upon decreasing the area; see Figure 4b. This is the most obvious difference in the behavior of dye 1 on water and the other salt solutions.

The reflection spectra on water and the salt solutions with the exception of KCl showed negligible changes with time after compressing the monolayers to areas between 0.34 and 0.24 nm^2 during 1 h. On 10 mM KCl, relaxation phenomena at constant area are clearly visible in changes in the reflection spectrum with time; see Figure 4c. Within the short relaxation time of 2 min after compressing the monolayer to the area $A = 0.28$ nm^2 (curve 2), the band with $\lambda_{max} = 405$ nm shifts to the blue with $\lambda_{max} = 375$ nm. Then, the intensity increases and becomes constant after about 15 min (curve 4). During this time period, the initial fwhm of 118 nm increased to about 132 nm, and the surface pressure decreased from 25 to 15 mN/m.

Brewster Angle Microscopy (BAM). Images of the dye 1 monolayers taken with the Brewster angle microscope MiniBAM reveal no structures on water or on 10 mM KF (not shown). In contrast, the topography visible in the BAM images indicates the formation of domains (Figure 5) on 10 mM aqueous solutions of (a) $KClO_4$ for an area of $A = 0.4$ nm^2, (b) KI for $A = 0.45$ nm^2, and (c) KCl for $A = 0.4$ nm^2 as well as (d) for $A = 0.24$ nm^2 after 2 min of relaxation at constant area. Dark and bright domains are observed on $KClO_4$ in the phase-transition region. In the presence of KI in the subphase, the BAM image shows anisotropic structures that may be attributed to domains of associates giving rise to the new band at 500 nm in the reflection spectra. In the case of KCl (Figure 5c), large dendritic domains with brightness varying within the domains, surrounded by the homogeneous phase, are observed. The growth of the domains during monolayer compression is correlated with an increase in the surface potential and a red shift of the main band in the reflection spectra. During monolayer relaxation at $A = 0.24$ nm^2, the topography changes with the formation of white spots of high intensity. Simultaneously, the surface pressure and the surface potential decrease, and a blue shift of the main band in the reflection spectra at 0.24 nm^2 (Figure 4d) is observed. These phenomena are attributed to the formation of a new anisotropic phase during relaxation.

Discussion

Isotherms. The surface pressure−area isotherms of dye 1 on water and 10 mM KF are of the liquid-expanded type and show a hardly detectable phase transition upon compression starting around $A = 0.6$ nm^2. This interpretation is supported by the fact that no domains are visible in the BAM images, although this lack of topographic differentiation might be due to the limited resolution of the MiniBAM (about 5 μm) and the small size of such domains. The electrostatic repulsion between the amphiphilic molecules due to the positive charge of the chromophores may be one reason for the existence of the liquid-expanded phase when the counterions are located in the electric double layer underneath the headgroups of dye 1. A phase transition from the liquid-expanded to the liquid-condensed phase upon compression with the nearly horizontal part of the $\pi-A$ isotherm is clearly observed in the cases of aqueous 10 mM $KClO_4$, KI, and KCl. Bright domains of the liquid-condensed phase surrounded by the dark liquid-expanded phase are seen in the BAM images (Figure 5). In the case of KI and KCl, the domains are anisotropic probably because of the tilt of the chromophores, which have a higher tendency to form ordered arrays than do the hydrocarbon chains with the variation of the azimuth within the domains, similar to domains with particular inner structure in the case of, for example, long chain fatty acids[44] or their ethyl esters.[45] This behavior has to be attributed to the effect of the anions on the interactions

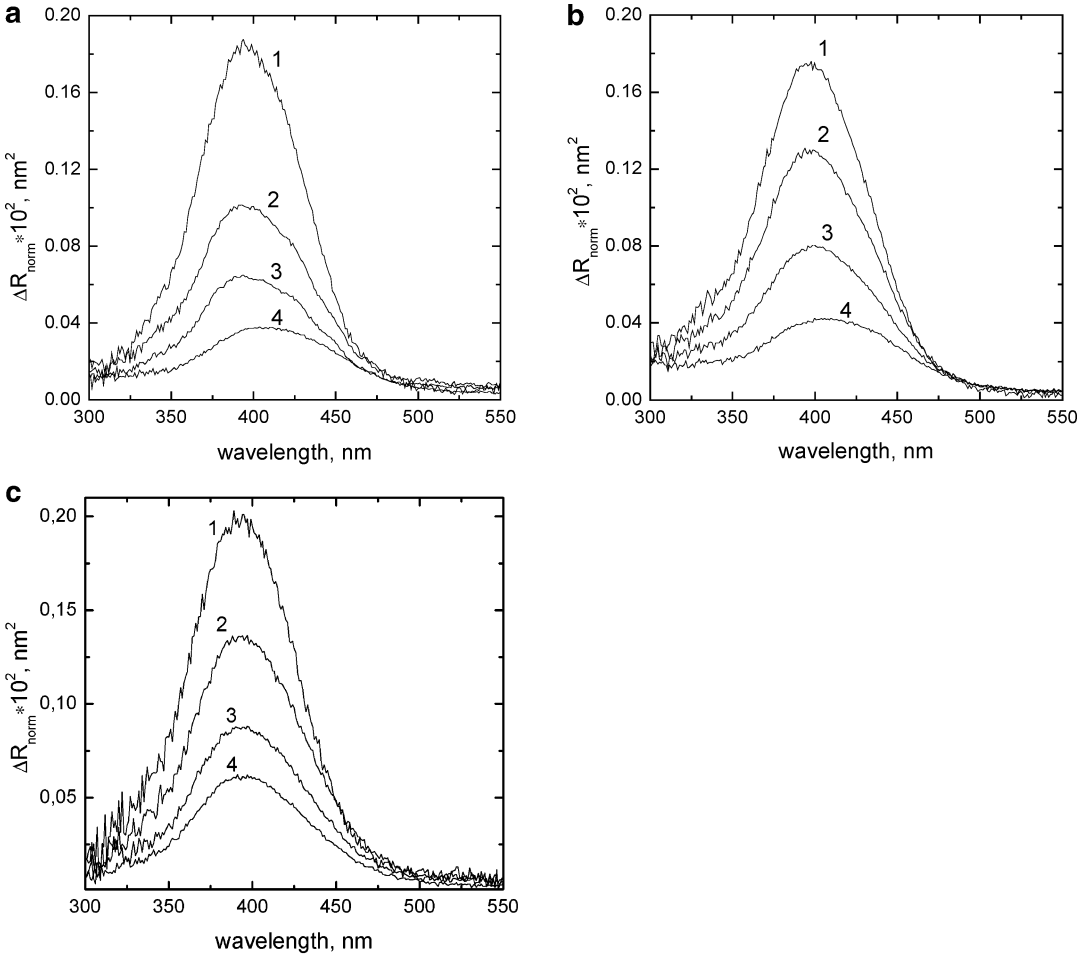

Figure 3. (a) Normalized reflection spectra of dye 1 on the water subphase at the following areas: 0.96 (1), 0.6 (2), 0.4 (3), and 0.26 (4) nm^2/molecule. (b) Normalized reflection spectra of dye 1 on the 10 mM $KClO_4$ solution at the following areas: 0.96 (1), 0.7 (2), 0.5 (3), and 0.34 (4) nm^2/molecule. (c) Normalized reflection spectra of dye 1 on the 10 mM KF solution at the following areas: 0.96 (1), 0.6 (2), 0.4 (3), and 0.28 (4) nm^2/molecule.

between the amphiphilic molecules. Considering the isotherms shown above in Figure 2, anions ClO_4^- and I^- interact more strongly than do the other anions with the chromophores. We propose that ClO_4^- and I^- are in close contact with the chromophores, presumably located in the monolayer headgroup region in the vicinity of the positive charge. Such a model is supported by the strongly reduced surface potential in comparison with that observed on pure water and on the aqueous solutions of the other salts.

According to recent molecular dynamics simulations of 1.5 M solutions of sodium halogenides in the absence of a monolayer,[46] ions such as iodide and bromide (and presumably perchlorate) are surface-active with their interfacial concentration being higher than in the bulk solution. In contrast, the concentration of Cl^- in the interfacial layer is only 30% of that in the bulk, and F^- and cations are repelled from the interface, leaving a layer of about 0.35 nm free of ions. It is reasonable to assume that in the presence of a monolayer of a cationic amphiphile (e.g., the dye 1) this interaction tendency between the interface and anions even increases and anions ClO_4^- and I^- are accumulated at the air/water interface and interact with dye 1 even at large area ($A > 1$ nm^2). As a consequence, the surface density of anions is then equal to the surface density of the positively charged dye molecules, and the resulting surface charge is zero. The rather abrupt increase in the surface potential upon compression at $A \approx 1$ nm^2 (Figure 2b, curves 3 and 4) may be related to a reorientation of the methoxy groups. Although the interactions of Cl^- with dye 1 are weaker than that of the highly polarizable anions, it differs considerably from F^- in modifying the behavior of dye 1 as documented in the BAM images and reflection spectra. However, the fact that surface pressure and surface potential in the presence 10 mM KF are larger than in the case of the pure water subphase is surprising because it seems to contradict the Gouy−Chapman theory of the electric double layer (EDL). However, one has to take into account the repulsion of F^- from the interface and the particular properties of the EDL in the case of dye 1. If the positive charge is localized on the pyridinium ring and the anion in the diffuse double layer, then the distance between the planes of positive and negative charge (thickness of diffuse double layer) is quite large; however, the space between the planes may have a low dielectric permittivity if it consists of a large fraction (styryl part) of dye molecules. This is true if the chromophores are not oriented parallel to the water surface but are more or less tilted. Evidence for such an orientation is provided by the surface potential−area isotherms. We assume that the chromophore has a ground-state dipole moment (in addition to the positive charge) that is oriented with the positive charge near the methoxy groups. If the chromophore becomes more tilted to the vertical upon monolayer compression, then the negative contribution of this dipole moment to the total apparent molecular dipole moment (normal component) should

(44) Overbeck, G.; Hönig, D.; Möbius, D. *Thin Solid Films* **1994**, *242*, 213.
(45) Weidemann, G.; Vollhardt, D. *Langmuir* **1996**, *12*, 5114.
(46) Jungwirth, P.; Tobias, D. J. *J. Phys. Chem. B* **2002**, *106*, 6361.

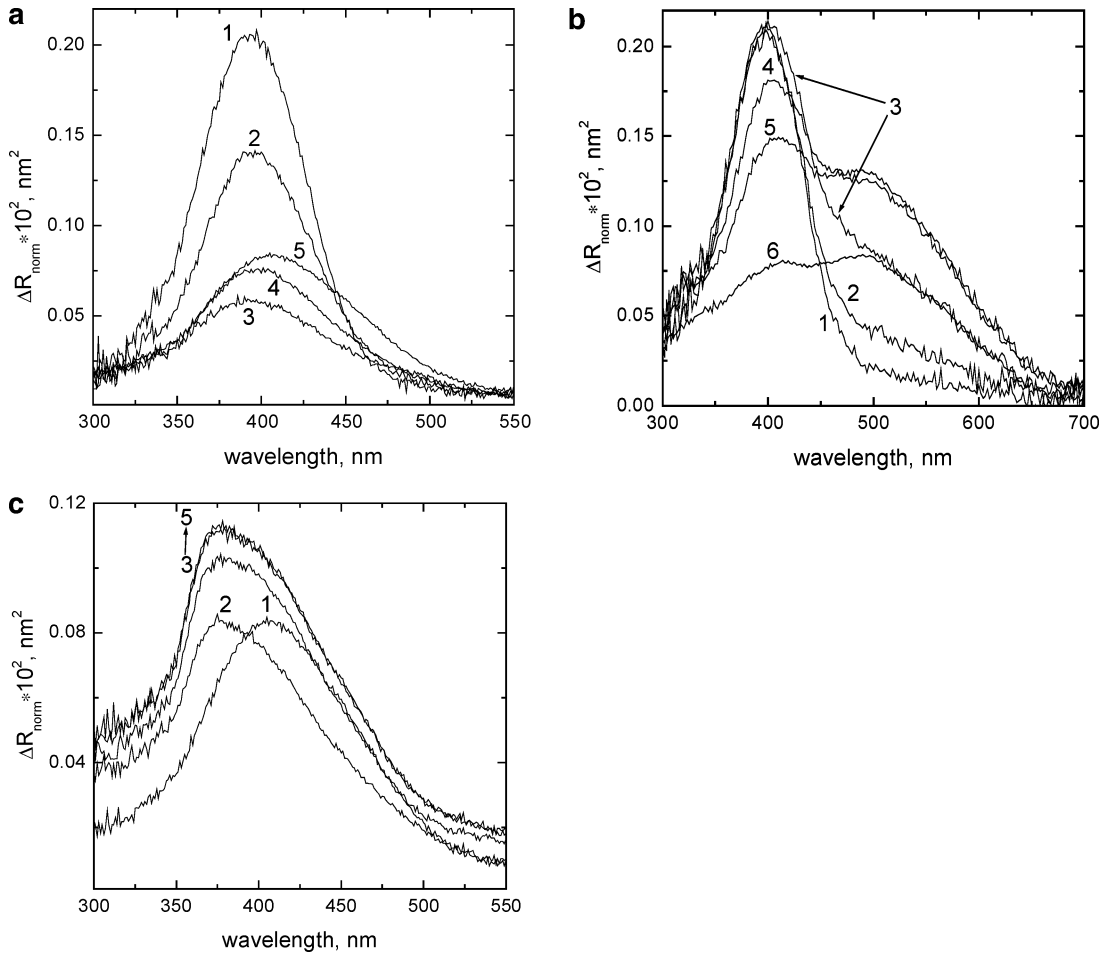

Figure 4. (a) Normalized reflection spectra of dye 1 on the 10 mM KCl solution at the following areas: 0.96 (1), 0.6 (2), 0.4 (3), 0.35 (4), and 0.24 (5) nm^2/molecule. (b) Normalized reflection spectra of dye 1 on the 10 mM KI solution at the following areas: 0.96 (1), 0.9 (2), 0.8 (3), 0.6 (4), 0.5 (5), and 0.34 (6) nm^2/molecule. (c) Normalized reflection spectra of dye 1 during monolayer relaxation on the 10 mM KCl solution at an area of 0.24 nm^2/molecule: initial state (1), 2 (2), 5 (3), 15 (4), and 30 (5) minutes.

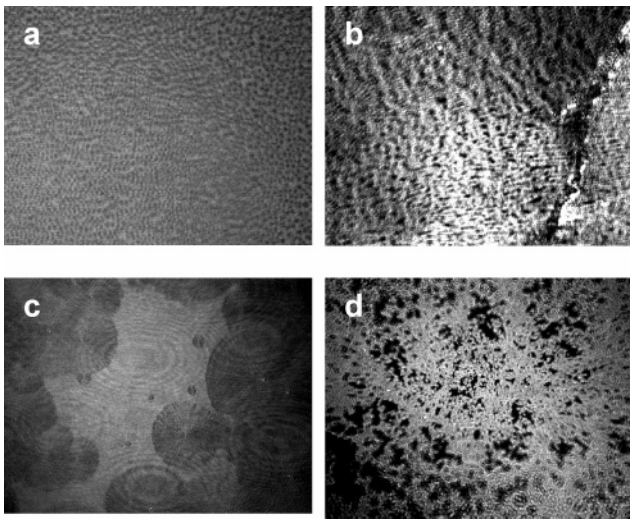

Figure 5. BAM images of dye 1 on the (a) 10 mM $KClO_4$ solution, (b) 10 mM KI solution, (c) 10 mM KCl solution at 0.4 nm^2, and (d) 10 mM KCl solution at 0.24 nm^2 after 10 min of relaxation.

become noticeable. According to the Helmholtz equation, the normal component of the apparent dipole moment is proportional to the surface potential normalized with respect to the surface density of the molecules, $\Delta V_{norm} = \Delta V \cdot A$. The contribution of the EDL, ΔV_{GC}, was calculated according to the Gouy−Chapman theory for a salt concentration of 3.2×10^{-6} M (water in equilibrium with air, pH 5.5) and a permittivity ϵ of 80

$$\Delta V_{GC} = \frac{2kT}{e} \sinh^{-1}\left[\frac{e\alpha}{A((5.88 \times 10^{-7})C\epsilon T)^{1/2}}\right] \qquad (1)$$

where α is the degree of dissociation of the monolayer headgroups ($\alpha = 1$ because the dyes are pyridinium salts), e is the electron charge, k is the Boltzmann constant, T is the absolute temperature, C is the ion concentration in moles/liter, A is the area per molecule. No charge compensation by counterions is considered.

Figure 6 shows an isotherm of ΔV_{GC} calculated from eq 1 as well as the difference $\Delta V_{exp} - \Delta V_{GC}$ (ΔV_{exp} taken from Figure 1, curve 4). In addition, the isotherm of the normalized surface potential difference (i.e., $(\Delta V_{exp} - \Delta V_{GC})A$) is shown. The decrease of this product with decreasing area supports the model of increasing tilt of the chromophores with monolayer compression.

The $\pi-A$ isotherms presented in Figures 1 and 2 clearly show that stable monolayers of dye 1 exist for areas that are much smaller than the area A_{max} of the flat-lying chromophore. Although this is often interpreted as evidence for a tilt of the chromophores, alternative arrangements have to be considered according to measurements of reflection spectra in most cases (e.g., the formation of dimers with one chromophore lying on top of the other). In the case of dye 1, $A_{max} = 0.72$ nm^2, whereas the minimum area is $A_0 = 0.33$ nm^2 (for chromophores oriented normal to the water surface without additional area for the anion).

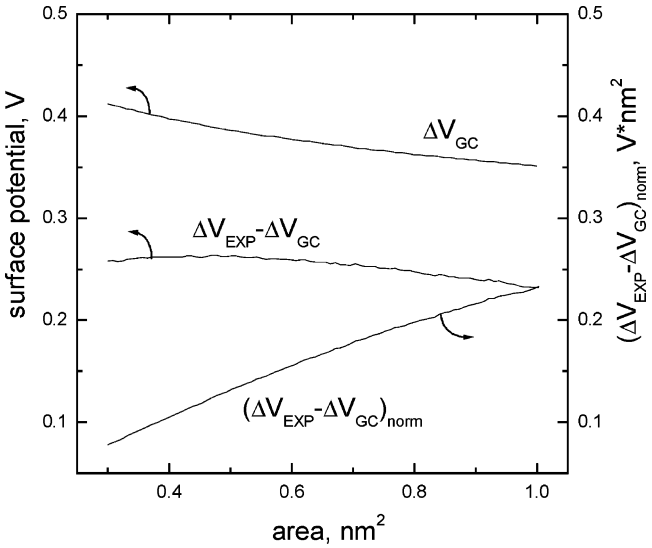

Figure 6. Calculated surface potencial−area isotherm for an electrical double layer (eq 1), the subtraction of this purely electrostatic contribution to the experimental isotherm for dye 2 in water (Figure 1, curve 4), and the last difference normalized by the area.

Chromophore Orientation and Environment. Isotherm measurements do not provide sufficient information about molecular organization in the dye monolayers. The reflection spectra shown in Figures 3 and 4 indicate changes in the orientation of the chromophores as well as their environment and association upon compression. In the presence of KF (Figure 3c), no change in the shape and position of the band is observed, and the normalized reflection ΔR_{norm} decreases upon reduction of the area. This has to be attributed to the increasing tilt of the transition moments and therefore of the chromophores. The tilt angle with respect to the surface normal may be evaluated from the integrated intensity. The reflection ΔR observed under normal incidence of light is given in a reasonable approximation by[42,47]

$$\Delta R = 2.303 \times 10^3 \Gamma f_{orient} \epsilon_D \sqrt{R_i} \quad (2)$$

where Γ is the surface concentration, $R_i = 0.02$, which the reflectivity of the air/water interface at normal incidence, ϵ_D the extinction coefficient of dye 1 in solution, and f_{orient} is a numerical factor that takes into account the different average orientation of the transition moment in solution as compared to the monolayer at the air/water interface. In the case of an orientation of the transition moments in the monolayer plane with a statistical distribution around the surface normal, $f_{orient} = 1.5$

$$f_{orient} = \frac{f_{app}}{f} \quad (3)$$

where f_{app}, the apparent oscillator strength, is determined from the measured reflection spectra according to

$$f_{app} = 2.6 \times 10^{-12} \int_{band} \Delta R_{norm} \, d\nu \quad (4)$$

with $\Delta R_{norm} = \Delta R/\Gamma$ and the oscillator strength f of the dye in solution

$$f = 1.44 \times 10^{-19} \int_{band} \epsilon_D \, d\nu \quad (5)$$

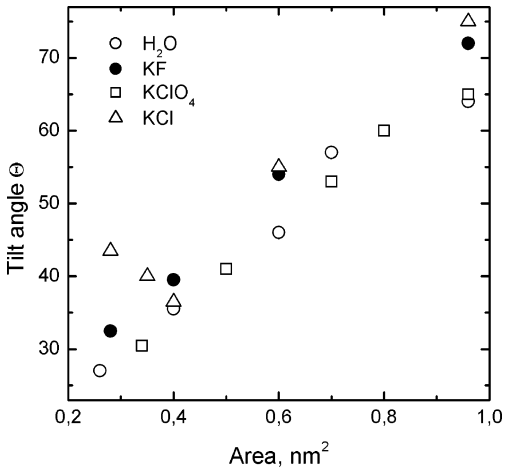

Figure 7. Polar tilt angle determined from normalized reflection measurements for dye 1 on water and 10 mM solutions of KF, $KClO_4$, and KCl.

For the general case with a statistical distribution of transition moments around the surface normal, the orientation factor is

$$f_{orient} = \frac{3}{2} \sin^2 \Theta \quad (6)$$

Here, Θ is the average tilt angle of the transition moments with respect to the surface normal. Thus, the polar tilt angle Θ may be calculated from the reflection spectra, providing information on the orientation of the chromophores. Figure 7 shows the values of the polar tilt angle (considering $f = 0.670$, the oscilatior strength value for dye 1 in acetonitrile solution) plotted versus area A for the subphase 10 mM aqueous solutions of KF (solid circles). The chromophores are tilted about 72° at $A = 0.96$ nm^2 and attain a polar tilt angle of about 30° at $A = 0.28$ nm^2. Although the reflection spectra change with respect to the shape and position of the maximum with compression in the cases of the subphase water and the other salt solutions, the same type of analysis has been applied, and the tilt angles obtained are represented in Figure 7 for water (circles), $KClO_4$ (squares), and KCl (triangles). In all cases, the tilt angle decreases continuously during monolayer compression from 65 to 75° at $A = 0.95$ nm^2 to about 30° at around $A = 0.3$ nm^2. As the molecules are approaching each other and become tilted upon compression, the environment of the chromophores becomes less polar and more polarizable. Therefore, different values of f were used for a more correct estimation of Θ in the case of the water, KCl, and $KClO_4$ solutions. The value $f = 0.670$ (acetonitrile solution) was used at $A > 0.4$ nm^2 in the polar environment, and $f = 0.782$ (chloroform solution) was used at $A < 0.4$ nm^2 in the nonpolar medium assumptions.

Our attempts to find a correlation between the maximum of the main band in the absorption and fluorescence spectra and the polar as well as nonpolar functions, given in ref 48 did not yield any reasonable correlations. In acetonitrile solution, the absorption maximum is at 398 nm, and a red shift is observed with decreasing solvent polarity. In highly polar solvents such as acetonitile and ethanol, the maximum of the absorption band is the same for dyes 1 and 2. Therefore, the amphiphilic cationic molecules are not interacting with the anions. In contrast, in solvents of low polarity the absorption maximum of dye 1 is red-shifted by about 6−7 nm as compared to that of dye 2. This phenomenon may be explained by assuming a strong interaction between the cationic

(47) Pedrosa, J.-M.; Romero, M. T. M.; Camacho, L.; Möbius, D. *J. Phys. Chem. B* **2002**, *106*, 2583.

(48) Yu, A.; Tolbert, C. A.; Farrow, D. A.; Jonas, D. M. *J. Phys. Chem. A* **2002**, *106*, 9407.

Scheme 1

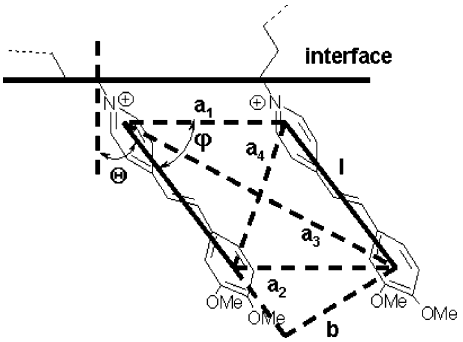

dyes and the anions. Anion ClO_4^- possesses a higher polarizability than Br^- [49] and decreases the energy of electronic transition. The polarizability of I^- is the largest in the range of anions investigated here, and we expect in this case the strongest red shift for the association of the anion and dye molecule. Irrespective of the type of anion, the polarizability of solvents of low polarity influences the spectroscopic properties of the solute. The largest red shift was found in solvents such as chloroform and dichloromethane. In contrast, solvents with rather low polarity and polarizability (e.g., tetrahydrofuran and ethyl acetate) lead to an increase in the energy of electronic transition.

The reflection spectra measured at large area ($A = 0.96$ nm^2) on water, 10 mM $KClO_4$, and 10 mM KF with a maximum at $\lambda_{max} = 395$ nm (Figure 3) closely resemble the absorption spectrum of dye 1 in acetonitrile. Upon compression, besides the decrease in the normalized reflection, a shoulder at longer wavelengths is observed in the case of water and 10 mM $KClO_4$ as the subphase, but not in the case of 10 mM KF. We conclude that anion F^- does not interact with the chromophores, whereas this is the case for ClO_4^-, which is also the anion on water. The situation is more complicated on the subphases containing 10 mM KCl and KI, and chromophore association has to be considered.

The shift of the band and the appearance of a new band in the reflection spectra may indicate medium effects and/or association of the chromophores forming dimers or larger aggregates. Because the chromophore presents solvatochromic effects (Table 1), a change in the environment due to monolayer compression and interactions with the anion may cause a shift of the band. At large areas after spreading, the molecules of dye 1 most probably are monomers (because of the electrostatic repulsion) located at the interface, with the chromophore partially immersed in a medium of rather high polarity and low polarizability that stabilizes the ground state of the chromophore. The compression of the monolayer leads to a decrease in intermolecular distances and causes changes in the dielectric properties of the interface. As a result, we should observe a red shift of the band and an increase in the oscillator strength because the chromophoric part of the close-packed monolayer may be considered to be a continuum with low dielectric permittivity and high polarizability. This conclusion is based on the spectral shift observed in bulk solutions by comparing acetonitrile and chloroform as solvents. The blue shift of the band with $\lambda_{max} = 420$ nm ($t = 0$ min) to 391 nm ($t = 15$ min) observed during monolayer relaxation on 10 mM KCl solution after compression to 0.24 nm^2 (Figure 4c) has a different origin and may be attributed to the formation of dimers or H aggregates.

Chromophore Association. Phenomena of association play an important role in monolayers of dyes at the air−water interface and on solid substrates.[41,50] In the simplest case of a sandwich dimer (in-phase oscillation of the transition moments), the absorption band shifts to shorter wavelengths. An out-of-phase oscillation of the transition moments resulting in a shift of the absorption band to longer wavelengths is optically forbidden. The shift of the absorption band is defined by the geometry and number of dyes in the associate.[51] According to the extended dipole model,[52,53] the energy of the optical transition of an aggregate of N chromophores is given by

$$\Delta E \approx \Delta E_{\text{monomer}} + \frac{2}{N}\sum_{i=1}^{N}\sum_{j=1}^{N} J_{ij} \tag{7}$$

$$J_{ij} = \frac{\delta^2}{4\pi\epsilon\epsilon_0}\left(\frac{1}{a_1} + \frac{1}{a_2} - \frac{1}{a_3} - \frac{1}{a_4}\right) \tag{8}$$

where J_{ij} is the interaction integral, δ is the charge of the transition dipole, $\epsilon = 2.5$ and ϵ_0 are the dielectric constants of the medium of the π electrons and of the vacuum, respectively, and the distances a_i are defined in Scheme 1. For simplicity, in this case we consider that all of the chromophore molecules in the associates have the same orientation (i.e., $a_1 = a_2$). The length of the transition dipole moment (l) was calculated for symmetrical cyanine dyes on the basis of quantum chemical calculations and experimental values of the transition dipole moment

$$M = \delta l = \left(\frac{3hfe^2 n\lambda_{max}}{8\pi m_e c_0}\right)^{1/2} \tag{9}$$

where δ is the charge of the transition dipole, h is Planck's constant, f is the oscillator strength, e is the electron charge, n is the refractive index of the solvent, λ_{max} is the wavelength of the absorption maximum, m_e is the electron mass, and c_0 is the speed of light in the vacuum. To simplify the calculations, Hans Kuhn recommends approximating l as about $^2/_3$ of the extension of the π-electron cloud,[51] which in our case gives rise to a value of $l = 0.85$ nm. The transition dipole moments $M = 8.74$ D (based on the spectrum in acetonitrile solution) and 10.07 D (chloroform solution) were calculated from the third term of eq 9. For the estimation of the distances a_i ($i = 1-4$), we have assumed that the minimum distance between two transition dipole moments (b) corresponds to twice the van der Waals radius of carbon (i.e., $b = 0.34$ nm).

In Figure 8, the absorption maximum (λ_{max}) calculated from eqs 7 and 8 is plotted against the tilt angle with respect to the water surface for a dimer ($N = 2$) as well as for associates of $N = 3$ and 4 chromophores. The two sets of curves refer to different environments of the chromophores determining the value of λ_{max}. The solid lines refer to a polar environment, and the dashed lines refer to a nonpolar, highly polarizable medium and were calculated using the values of M and the absorption maximum of the monomer obtained from the spectra measured in acetonitrile and chloroform solutions, respectively. For example, the experimental $\lambda_{max} = 375$ nm in the case of relaxed dye 1 on 10 mM KCl is in good agreement with the values calculated for a nonpolar environment, $N = 4$, and a polar tilt angle of $\Theta = 30°$. In the case of the 10 mM KI solution, we

(49) Kunz, W.; Belloni, L.; Bernard, O.; Ninham, B. W. *J. Phys. Chem. B* **2004**, *108*, 2398.

(50) Kuhn, H.; Möbius, D. Monolayer assemblies. In *Investigations of Surfaces and Interfaces*, 2nd ed.; Rossiter, B. W., Baetzold, R. C., Eds.; John Wiley & Sons: New York, 1993; Vol. IXB, pp 375−542.

(51) Kuhn, H.; Kuhn, C. Chromophore Coupling Effects. In *J-aggregates*; Kobayashi, T., Ed.; World Scientific: Singapore, 1996; pp 1−40.

(52) Czikkely, V.; Försterling, H. D.; Kuhn, H. *Chem. Phys. Lett.* **1970**, *6*, 207.

(53) Saito, K.; Ikegami K.; Kuroda, S.; Tabe, Y.; Sugi, M. *Jpn. J. Appl. Phys.* **1991**, *30*, 1836.

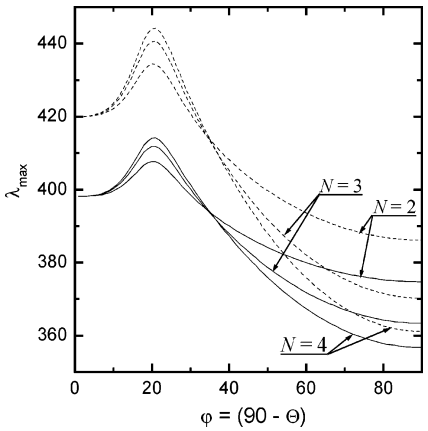

Figure 8. Dependence of λ_{max} on the polar tilt angle and number of chromophores in aggregates of 2, 3, and 4 chromophores for two types of environments: solid lines − polar medium (the position of the absorption maximum and the oscillator strength in acetonitrile solution were used for the calculations); dashed lines − nonpolar, highly polarizable medium (the position of the absorption maximum and the oscillator strength in chloroform solution were used for the calculations).

assume that the chromophores are nearly untilted and largely in contact with water. Because of the appearance of the new band at longer wavelengths, the apparent oscillator strength even increases with compression until the area $A = 0.5$ nm^2 is reached. Even with a large number of chromophores arranged as in J aggregates, the experimentally observed $\lambda_{max} = 500$ nm (after deconvolution of the spectra in Figure 4b using two Gaussian functions) is not obtained theoretically. Therefore, we conclude that additional interactions give rise to the new band at longer wavelengths. It may be worth mentioning that this band is also observed for the analogue styryl-pyridinium dye with 18-crown-6 instead of the two methoxy groups on 10 mM KI solution, whereas the dye without methoxy groups but a methylthio group in the para position of the styryl moiety does not show this band with a maximum around 500 nm (unpublished results).

Conclusions

Anions in the aqueous subphase influence the surface behavior of amphiphilic cationic styryl-pyridinium dye 1 according to the Hofmeister series. Examples of the phase transition are observed in the surface pressure−area isotherms as well as the surface potential. Upon compression, the chromphores become more and more tilted, and the changes in the reflection spectra indicate changes in the chromophore environment as well as in chromophore association. In particular, a new band shifted to shorter wavelengths with respect to the band of the dye monomer after monolayer relaxation on 10 mM aqueous KCl solution is attributed to tetramers with a tilting angle of about 30°. The origin of the new band observed in the presence of I^- ions at longer wavelengths than for the monomer band is not completely clear because model calculations assuming the formation of extended two-dimensional J aggregates did not yield the observed shift.

Acknowledgment. D.M. gratefully acknowledges the financial support of the Fonds der Chemischen Industrie, Germany. S.Yu.Z. is thankful to the Alexander von Humboldt Stiftung (Germany) for the research fellowship.

LA051942Q